PHYSICAL REVIEW C VOLUME 20, NUMBER 2 AUGUST 1979

Unified shell-model description of nuclear deformation

P. Federman
Instituto de Fisica, Universidad Nacional Autonoma de Mexico, Apartado Postal 20-364, Mexico 20, D. F.

S. Pittel
Bartol Research Foundation of the Franklin Institute, University of Delaware, Newark, Delaware 19711
(Received 19 March 1979)

A unified shell-model description of nuclear deformation valid throughout the periodic table is presented. Microscopic calculations for the Zr and Mo isotopes are carried out in the frameworks of the shell model and the Hartree-Fock-Bogoliubov method, respectively, to study the shape transition in these nuclei. It is shown that deformation is produced by the isoscalar component of the neutron-proton (n-p) interaction in this region, as in the lighter ($2s,1d$)-shell region. Deformation sets in when the $T = 0$ n-p interaction dominates over the sphericity-favoring pairing interaction between $T = 1$ pairs of nucleons. When shell effects are important, as for the light and medium-weight regions mentioned above, the simultaneous occupation of neutrons and protons of spin-orbit "partner" orbitals plays a crucial role in determining the onset of deformation. However, their effect is probably less important in the rare-earth and transuranic regions due to the rapid accumulation of single-particle orbitals.

NUCLEAR STRUCTURE Microscopic description of nuclear deformation; shell-model calculations of ^{96}Zr, ^{98}Zr, and ^{100}Zr; HFB calculations of ^{98}Mo–^{110}Mo; discussion of light and heavy deformed nuclei; relation to interacting boson approximation.

I. INTRODUCTION

Since the discovery of the first regions of nuclear deformation for transuranic and rare-earth heavy nuclei in the early 1950's, several additional deformed regions have been discovered throughout the periodic table. Deformation was also observed for light nuclei in the ($2s$, $1d$)-shell region and more recently for medium-weight nuclei around the Zr and Mo isotopes.[1]

The collective and unified models have had considerable success in giving a description of deformation in heavy nuclei by introducing a phenomenological long-range residual quadrupole-quadrupole interaction between all nucleons.[2] On the other hand, also in the early 1950's but from a shell-model point of view, deShalit and Goldhaber suggested that collective effects such as the lowering of the first excited $J = 2^+$ level in even-even nuclei could be produced by the isoscalar residual interaction between neutrons and protons.[3] They showed that the neutron-proton (n-p) interaction is responsible for strong mixing of shell-model configurations, a necessary condition for deformation. The mechanism by which this occurs is traced back to the strong overlap between neutron and proton orbitals, particularly when they satisfy the conditions $n_n = n_p$ and $l_n \approx l_p$.[3]

The discovery of a region of deformed light nuclei in the ($2s$, $1d$) shell motivated microscopic studies that further support the above picture. Talmi and Unna showed that the strong shell-model configuration mixing necessary to produce deformation in the ($2s$, $1d$) shell could be traced to the strong isoscalar residual interaction between neutrons and protons when they occupy the spin-orbit "partner" orbitals $1d_{5/2}$ and $1d_{3/2}$.[4] These orbits certainly satisfy the condition $n_n = n_p$ and $l_n \approx l_p$.

Recent Hartree-Fock-Bogoliubov (HFB) calculations show that in neutron-rich nuclei also, deformation appears when the residual isoscalar neutron-proton correlations dominate over the $T = 1$ pairing correlations.[5,6] This conclusion is also supported by the fact that all known deformed nuclei have open shells of both neutrons and protons.

Within the ($2s$, $1d$) region the importance of the n-p interaction in producing deformation can be appreciated by comparing the experimental energy spectra of ^{20}Ne and ^{20}O (see Fig. 1). While ^{20}Ne exhibits a ground-state rotational band, the low-lying spectrum of ^{20}O shows no similar collective trend. Rather it can be understood in terms of simple shell-model configurations.[4] Moreover, the isoscalar n-p interaction is also responsible for the appearance of core-excited deformed states in mass-16 and mass-18 nuclei, providing the large extra binding necessary to compensate for the respective $4\hbar\omega$ and $2\hbar\omega$ losses in single-particle energy.[8]

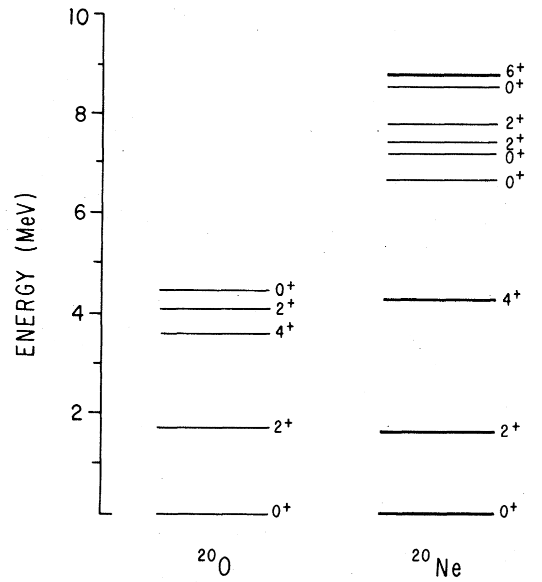

FIG. 1. Experimental spectra of ^{20}O and ^{20}Ne, from Ref. 7. In the ^{20}Ne spectrum, heavy lines denote levels belonging to the ground-state rotational band.

Thus, the emerging microscopic picture is one in which deformation is produced by the $T=0$ part of the n-p residual interaction, rather than by a long-range quadrupole-quadrupole interaction.

In this work we study the mechanism by which nuclear deformation is produced by focusing on the region of deformed Zr and Mo isotopes. The nuclei in this region have the advantages of being both neutron-rich like the heavy deformed nuclei and still amenable to shell-model investigation. We show that the above picture based on n-p correlations is valid also in this region. Our conclusions provide a unified description of nuclear deformation that seems to be valid for all regions of the periodic table. The emerging description is one in which deformation indeed arises for all nuclei from the n-p residual interaction, more specifically from its isoscalar component. It is this interaction that produces the strong spatial correlations (or configuration mixing) necessary to produce deformation. We also discuss the connections with recent microscopic efforts for heavy deformed nuclei in the framework of the interacting boson approximation[9] (IBA) as well as early $(2s, 1d)$-shell efforts for light nuclei.[4] In light- and medium-weight nuclei, where shell effects are important, the simultaneous occupation by neutrons and protons of selected orbitals such as the spin-orbit partners plays a crucial role in determining where deformation occurs.[6,10,11] Their effect may be less important in heavier regions, owing to the rapid accumulation of single-particle orbitals.

In Sec. II we review the experimental data for the Zr isotopes and discuss them qualitatively. A detailed shell-model calculation to study the shape transition that occurs between ^{96}Zr and ^{100}Zr is presented in Sec. III. Section IV is devoted to the Mo isotopes, and in Sec. V we discuss the connections between our results in the Zr-Mo region and other deformed regions. In Sec. V, we also discuss our picture in relation to the interacting boson approximation and summarize our principal conclusions.

II. ENERGY SYSTEMATICS OF THE ZIRCONIUM ISOTOPES

The positive-parity energy spectra for all the Zr isotopes from $A=96$ to $A=102$ are presented in Fig. 2. The experimental situation up to $A=96$ was quite well known, and also quite well understood in terms of simple spherical shell-model configurations, for a number of years.[12] On the other hand, the data for $A=98$, 100, and 102 only recently became available when fission fragments were analyzed with modest but quite ingenious experimental facilities.[1,13,14] As can be seen in Fig. 2, the energy-level systematics exhibit several striking features. First of all, the data exhibit a clear and smooth shape transition as a function of the neutron number. The transition from simple shell-model spectra to an excellent axially symmetric rotor is quite complete by ^{102}Zr, namely for $N=62$. Moreover, the shape transition is accompanied by a lowering of the first excited $J=0^+$ level. Up to ^{96}Zr this level appears roughly at 1.5 MeV in all the isotopes. In ^{96}Zr it appears at 1.59 MeV, but in ^{98}Zr it drops dramatically to almost half that value, to 0.85 MeV. In ^{100}Zr it drops even further to 0.33 MeV or perhaps to become the ground

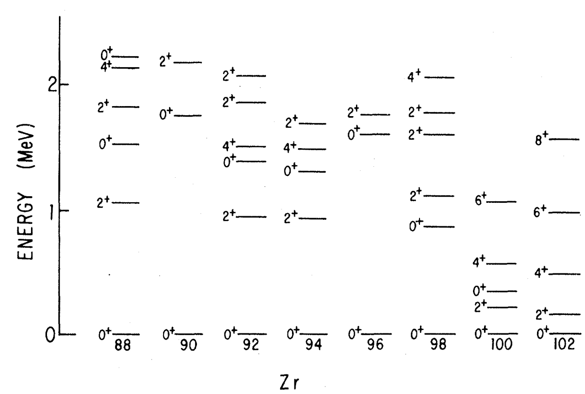

FIG. 2. Experimental spectra of positive-parity energy levels for the Zr isotopes from $N=48$ to $N=62$, from Refs. 1, 13, and 14.

state.[5]

Let us now see what the shell model can qualitatively tell us about this region of deformation. In Fig. 3, the relevant single-particle levels are shown. They are discussed in the next section. While neutrons and protons added to ^{88}Sr do not fill the same orbitals, they can simultaneously fill the $1g_{9/2}$ proton and $1g_{7/2}$ neutron spin-orbit partner orbitals, equivalent to the $1d_{5/2}$ and $1d_{3/2}$ in the $(2s, 1d)$-shell region. According to the deShalit-Goldhaber rule, the good overlap of these orbitals could lead to strong spatial n-p correlations. In analogy with the situation in the $(2s, 1d)$ shell, these n-p correlations most likely provide the mechanism for deformation in the heavy Zr isotopes.[10,11]

Let us now discuss qualitatively how the strong attraction between $1g_{9/2}$ protons and $1g_{7/2}$ neutrons can lead to deformation in these isotopes. In a purely independent-particle picture of the Zr isotopes, the $1g_{9/2}$ proton orbital is completely empty and the $1g_{7/2}$ neutron orbital does not begin to fill until after $N = 62$. The residual interaction between valence nucleons modifies this picture. For example, the n-n and p-p interactions distribute nucleons over all the active orbitals by configuration mixing, as illustrated by the fact that ^{90}Zr has a roughly 30% $(1g_{9/2})^2$ admixture in its ground-state wave function.[15] These pairing correlations stabilize the spherical shapes. On the other hand, sufficiently strong n-p interactions can break down the pairing correlations by a polarization mechanism. For example, adding neutrons to the $1g_{7/2}$ orbital can cause some of the protons in the $2p_{1/2}$ orbital to be promoted into the $1g_{9/2}$ orbital because of the large $1g_{9/2}$-$1g_{7/2}$ isoscalar residual interaction. The increased occupation of the $1g_{9/2}$ proton orbital can, in turn, polarize the neutrons, promoting

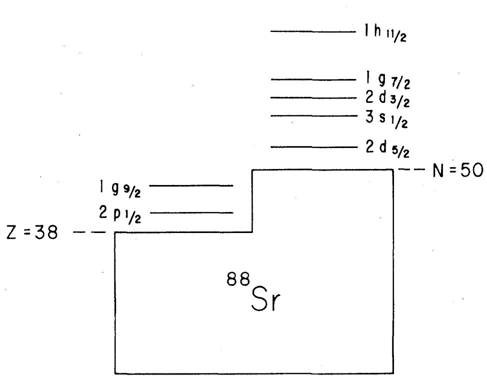

FIG. 3. Single-particle levels appropriate to a description of nuclei in the Zr-Mo region. An ^{88}Sr core is assumed.

additional ones into the $1g_{7/2}$ orbital. Such mutual polarization can only occur if the gain in n-p interaction energy exceeds the loss in single-particle plus pairing energy. In this way, the pairing correlations can be gradually broken down and replaced by spatial correlations between neutrons and protons. Once the spatial n-p correlations become dominant, the system deforms.

There is experimental evidence to support such a polarization mechanism in this region. Neutron stripping data on ^{88}Sr, ^{90}Zr, and ^{92}Mo indicate that as the $1g_{9/2}$ proton orbital is filled, the $1g_{7/2}$ neutron orbital comes down in energy, from 2.67 MeV in ^{89}Sr (Ref. 16) to 2.19 MeV in ^{91}Zr (Ref. 17) to 1.37 MeV in ^{93}Mo.[18]

In the next section we describe shell-model calculations that support the above picture. Thus, the same physics seems to underlie deformation, both in the $(2s, 1d)$ shell and in the neutron-rich Zr isotopes. In both regions, deformation seems to result from strong n-p correlations which develop when neutrons and protons simultaneously fill selected partner orbitals.[10]

III. THE SHAPE TRANSITION IN THE ZIRCONIUM ISOTOPES

In this section, we present the results of shell-model calculations for ^{96}Zr and ^{98}Zr and the $J = 0^+$ levels of ^{100}Zr, performed in order to study the shape transition in the Zr isotopes. At least for now, these are the only neutron-rich nuclei in which a shape transition is amenable to shell-model investigation.

To keep the sizes of the Hamiltonian matrices manageable, an inert ^{94}Sr core was assumed. This assumption seems quite reasonable in view of the "closure" effect exhibited by the ^{96}Zr spectrum (see Fig. 2). The valence neutrons are restricted to the $3s_{1/2}$, $2d_{3/2}$, and $1g_{7/2}$ orbitals and the valence protons to the $2p_{1/2}$, $1g_{9/2}$, and $2d_{5/2}$ orbitals. The dimensions of the Hamiltonian matrices involved in the ^{98}Zr calculations are 35, 115, and 145 for the $J = 0^+$, 2^+, and 4^+ states, respectively. The $J = 0^+$ matrix for ^{100}Zr is of dimension 226.

The calculations were performed with no free parameters. We used the same Yukawa force with Rosenfeld mixture as was used for ^{88}Sr.[19] The single-particle splittings were taken from the spectra of ^{89}Sr (Ref. 16) and ^{89}Y (Ref. 20), and assumed to also apply to a ^{94}Sr core, as discussed in Ref. 5. These splittings are listed in Table I. The calculations were performed using the Oak Ridge-Rochester shell-model code.

The first excited $J = 0^+$ level in ^{96}Zr is calculated at 1.46 MeV to be compared with the experimental value of 1.59 MeV, and contains 81% of the $1g_{9/2}{}^2$

TABLE I. Single-particle energies for Zr shell-model calculations.

Protons		Neutrons	
Orbital	Energy (MeV)	Orbital	Energy (MeV)
$2p_{1/2}$	0.0	$3s_{1/2}$	0.0
$1g_{9/2}$	0.89	$2d_{3/2}$	1.13
$2d_{5/2}$	4.50	$1g_{7/2}$	1.64

configuration. Analogously, the ground state has 80% of the $2p_{1/2}^2$ configuragion, in agreement with proton stripping data.[15] The calculated spectrum of ^{98}Zr is shown in Fig. 4, together with the assigned experimental levels. The energy spectrum is well reproduced, including the dramatic lowering of the first $J=0^+$ excited state relative to the lighter Zr isotopes.

In order to understand how this lowering effect occurs, a weak-coupling analysis of the ^{98}Zr eigenstates was performed in terms of the two-neutron eigenstates of ^{96}Sr coupled to the two-proton eigenstates of ^{96}Zr:

$$\Psi_\alpha^{J=0}(^{98}\mathrm{Zr}) = \sum_{\substack{J' \\ ik}} C^\alpha_{ikJ'}[\Phi_i^{J'}(^{96}\mathrm{Sr})\Phi_k^{J'}(^{96}\mathrm{Zr})]^{J=0}. \qquad (1)$$

Here the square bracket denotes the coupling of the angular momenta J' and J' to total angular momentum $J=0$.

The percentages of the principal weak-coupling components for the first four $J=0^+$ states of ^{98}Zr are presented in Table II. A shorthand notation $J_i \times J_k$ is used to denote the coupling of the ith two-neutron eigenstate with angular momentum J to the kth two-proton eigenstate with the same angular momentum J.

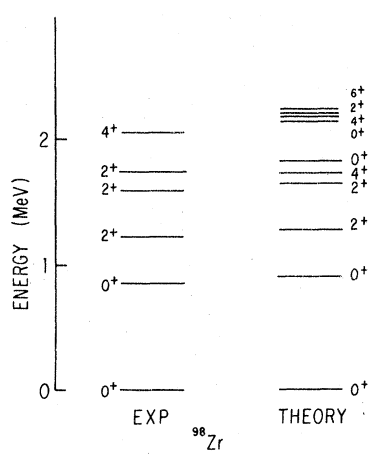

FIG. 4. Calculated and experimental positive-parity levels for ^{98}Zr. Only those experimental levels with firm spin assignments are shown.

The results are quite striking. The ground state remains almost pure (96%) $0_1 \times 0_1$, whereas the first excited 0^+ state is very strongly admixed. Actually, the first excited 0^+ state seems to be the only one very strongly admixed.

These results can be understood by considering the structure of the parent states in ^{96}Zr. As noted above, the ground state of ^{96}Zr has its two valence protons in the $2p_{1/2}$ orbital roughly 80% of the time, with small admixtures of other configurations. The neutron-proton interaction is not very effective for protons in the $2p_{1/2}$ orbital. Thus, when two neutrons are added to the ^{96}Zr ground state, the corresponding state in ^{98}Zr (namely the ground state) remains very pure. In the case of the first excited 0^+ state of ^{96}Zr, for which 80% of the valence protons are in the $1g_{9/2}$ orbital, the situation is very different. Since the valence neutrons can (at least in part) fill the $1g_{7/2}$ orbital, the neutron-proton interaction starts to be strongly exploited. The effect of the interaction between the $1g_{9/2}$ and $1g_{7/2}$ partner orbitals is to lower dramatically the energy of the 0_2^+ level in ^{98}Zr and, at the same time, to induce strong configuration mixing in the resulting wave function.

Since the ^{96}Zr and ^{96}Sr eigenstates correspond to spherical shapes, any ^{98}Zr state with a rather pure weak-coupling structure also corresponds to a spherical shape. Only by admixing many weak-coupled configurations can a deformed state be generated from such a basis. Thus, the first excited 0^+ state of ^{98}Zr seems the natural candidate to foster the deformed ground state of ^{100}Zr.

To see whether this is indeed the case, we have also carried out a shell-model calculation of the $J=0^+$ levels in ^{100}Zr. In Table III we present the energies and the weak-coupling structure for the first two $J=0^+$ states. The first excited $J=0^+$ level is calculated at 0.62 MeV, further lowered with respect to ^{98}Zr, and in reasonable agreement with the experimental value of 0.33 MeV.[14] Here the weak-coupling analysis involves the coupling of the four-neutron eigenstates of ^{98}Sr to the two-proton eigenstates of ^{96}Zr:

$$\Psi_\alpha^{J=0}(^{100}\mathrm{Zr}) = \sum_{\substack{J' \\ ik}} D^\alpha_{ikJ'}[\Phi_i^{J'}(^{98}\mathrm{Sr})\Phi_k^{J'}(^{96}\mathrm{Zr})]^{J=0}. \qquad (2)$$

Again, the shorthand notation $J_i \times J_k$ is used to denote the coupling of the ith four-neutron eigenstate with angular momentum J to the kth two-proton eigenstate with the same angular momentum. The situation is now reversed with respect to ^{98}Zr. It is the first excited state that contains the largest component (55%) of the $0_1 \times 0_1$ configuration, while the "collective" ad-

TABLE II. Weak-coupling percentages for the first four $J=0^+$ states in ^{98}Zr in terms of the $^{96}Sr \otimes {}^{96}Zr$ states. The notation is explained in the text.

Energy (MeV)	$0_1\times0_1$	$0_2\times0_1$	$0_3\times0_1$	$0_1\times0_2$	$0_2\times0_2$	$0_3\times0_2$	$2_1\times2_1$	$2_2\times2_1$	$2_3\times2_1$	$2_4\times2_1$	$4_1\times4_1$	$4_2\times4_1$	$4_3\times4_1$
0.0	96.1	0.7	0.1	0.3	0.3	0.3	0.6	0.2	0.2	0.3	0.2	0.1	0.1
0.90	1.8	11.9	7.4	16.9	10.5	12.6	2.8	4.1	3.9	12.8	1.0	1.5	5.4
1.82	0.8	9.0	2.4	70.2	0.4	4.5	2.8	0.3	0.3	4.5	1.0	0.0	1.5
2.08	0.1	68.3	13.9	0.4	3.3	4.2	0.4	0.4	0.0	6.2	0.0	0.1	1.4

mixture of shell-model configurations appears for the ground state.

As can be seen in Tables IV and V, the calculated occupation numbers for ^{98}Zr and ^{100}Zr provide further confirmation of the crucial role of the $1g_{9/2}$ and $1g_{7/2}$ partner orbitals in producing the correlations required for deformation in these isotopes. In ^{98}Zr the $J=0^+$ state with the largest number of $1g_{9/2}$ protons and $1g_{7/2}$ neutrons is the highly coherent 0_2^+ state. Similarly, in ^{100}Zr the deformed ground state is dominated by $1g_{9/2}$ protons and $1g_{7/2}$ neutrons. Thus, the deformed ground state of ^{100}Zr (and presumably of the heavier Zr isotopes) seems to have its parentage in the first excited 0^+ state of the lighter isotopes. In view of the present description, we would expect that in ^{102}Zr, after the crossing has taken place, the first excited $J=0^+$ level would go up in energy. Unfortunately, the low cross sections make the experimental search for the first excited $J=0^+$ state in ^{102}Zr very difficult.[21]

The role of the $1g_{9/2}$ orbitals in producing configuration mixing, and thus deformation in the Zr isotopes, can be made even clearer by considering the effects of varying the energies of the $1g_{7/2}$ and $2d_{3/2}$ neutron orbitals in the calculations. This has been done for the $J=0^+$ levels of ^{98}Zr. The results are quite insensitive to changes in the $2d_{3/2}$ single-particle energy. There is no sizable effect for an increase of 0.5 MeV, and an increase 10 times larger, namely, of 5.0 MeV, lifts the energy of the first excited $J=0^+$ state in ^{98}Zr from 0.9 MeV to only 1.1 MeV. In dramatic contrast, when $\epsilon(1g_{7/2})$ is increased by only 0.5 MeV, the energy of the first excited $J=0^+$ level goes from 0.9 to 1.4 MeV. The effect is even more apparent in the wave functions. The largest component of the calculated 0_2^+ state, which is only 17% of the $0_1\times0_2$ configuration in Table II, becomes 49% when $\epsilon(1g_{7/2})$ is lifted by 0.5 MeV and 71% when it is lifted by 1.0 MeV.

It is interesting to ask whether an excited rotational band already exists in ^{98}Zr based on the 0_2^+ level as its band head.[22] Situations of this type are well known in the $(2s, 1d)$ region and will be discussed in Sec. V. The results of weak-coupling analyses of the $J=2^+$ and 4^+ wave functions of ^{98}Zr show no evidence of such a rotational band. The energies of the most "collective" states of each spin and parity are 0.90 MeV for $J=0^+$, 2.21 MeV for $J=2^+$, and 2.20 MeV for $J=4^+$ (see Fig. 4). Thus, the present results suggest that in the Zr isotopes the rotational band gradually develops as neutrons are added.

It is of great interest to calculate the $J=2^+$ and 4^+ levels in ^{100}Zr to see whether the model space under discussion is indeed capable of fully developing a rotational band. The matrices involved in those calculations are very large, with dimensionalities of 920 and 1253 for $J=2^+$ and 4^+, respectively. Such calculations are currently underway, making use of the Lanczos algorithm for diagonalizing large matrices.[23]

IV. THE SHAPE TRANSITION IN THE Mo ISOTOPES

The positive-parity spectra for all the Mo isotopes from $A=92$ to $A=104$ are presented in Fig. 5.[1,24] As for the Zr isotopes, the data exhibit a smooth shape transition as a function of the neutron number. The transition from simple shell-model spectra to rotational spectra is, as in the Zr isotopes, completed by $N=62$, namely for ^{104}Mo.

TABLE III. Weak-coupling percentages for the first two $J=0^+$ states in ^{100}Zr in terms of the $^{98}Sr \otimes {}^{96}Zr$ states. The notation is explained in the text.

Energy (MeV)	$0_1\times0_1$	$0_2\times0_1$	$0_1\times0_2$	$0_2\times0_2$	$2_1\times2_1$	$2_2\times2_1$	$2_3\times2_1$	$4_1\times4_1$	$4_2\times4_1$
0.0	39.2	6.1	6.0	11.8	4.2	4.1	11.8	1.6	4.7
0.62	54.6	12.2	13.8	5.5	0.2	0.9	7.3	0.2	2.3

TABLE IV. Occupation numbers of single-particle orbitals for ^{98}Zr $J=0^+$ states.

Energy	Neutron orbitals			Proton orbitals		
(MeV)	$3s_{1/2}$	$2d_{3/2}$	$1g_{7/2}$	$2p_{1/2}$	$1g_{9/2}$	$2d_{5/2}$
0.0	1.81	0.12	0.08	1.63	0.34	0.03
0.90	0.33	0.28	1.39	0.25	1.67	0.08
1.82	1.52	0.18	0.31	0.29	1.68	0.03
2.08	0.09	1.63	0.28	1.47	0.50	0.03

Because of the increased number of valence protons relative to the Zr isotopes, the Mo isotopes are much more difficult to study in a shell-model framework. We have, therefore, studied their shape transition in the simpler framework of the Hartree-Fock-Bogoliubov (HFB) method.[25] This method has the desirable feature of including both deformation-producing effects (through the Hartree-Fock field) and sphericity-producing effects (through the pairing field), with both fields generated in a self-consistent fashion by the same effective two-nucleon interaction.

A good indicator within the HFB method of the tendency of a nucleus to deform is the difference between the binding energies associated with the spherical and deformed shapes (the deformation energy). For each nucleus we performed the calculations for spherical, prolate, and oblate shapes. The largest binding energy determines the preferred shape. If the deformation energy is sufficiently large, the nucleus can sustain permanent deformation.

For these calculations the active orbitals listed in Table I were expanded to include the $1h_{11/2}$ neutron orbital, for which a single-particle energy of 3.0 MeV above the $3s_{1/2}$ orbital was assumed.[5] The remaining single-particle splittings were the same as in Table I. The residual interaction for this study was assumed to be a surface delta interaction (SDI).[26] The SDI contains two parameters A_0 and A_1, which define the strengths of the isoscalar and isovector parts of the interaction, respectively. With the choice of parameters $A_0=0.6$ MeV and $A_1=0.35$ MeV, this interaction reproduces, fairly well, effective-interaction matrix elements for this region.[12,27]

TABLE V. Occupation numbers of single-particle orbitals for ^{100}Zr $J=0^+$ states.

Energy	Neutron orbitals			Proton orbitals		
(MeV)	$3s_{1/2}$	$2d_{3/2}$	$1g_{7/2}$	$2p_{1/2}$	$1g_{9/2}$	$2d_{5/2}$
0.0	1.82	0.80	1.39	0.42	1.48	0.10
0.62	1.89	1.55	0.55	1.45	0.53	0.02

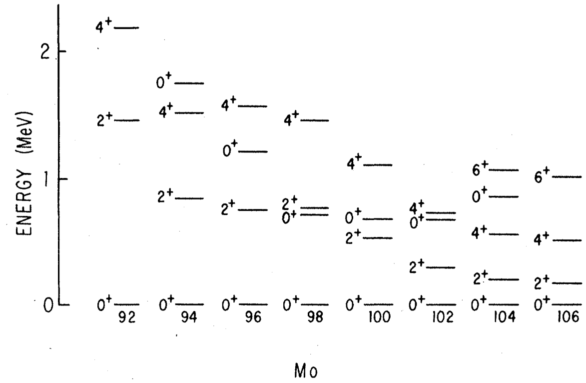

FIG. 5. Experimental spectra of positive-parity energy levels for the Mo isotopes from $N=50$ to $N=64$, from Refs. 1 and 24.

In order to investigate which component of the nuclear force produces deformation in these isotopes, we performed the calculations for various sets of values of the parameters A_0 and A_1. The resulting prolate deformation energies are summarized in Tables VI and VII. Only the prolate results are presented since all the calculations favor such a solution.

Table VI shows the results of varying A_0 while holding A_1 fixed. For small values of A_0 there is no tendency toward deformation in any of the isotopes studied. Suddenly, however, a critical value of A_0 is reached, above which the deformation energy increases very rapidly with increasing A_0.

The results obtained when A_0 was kept fixed and A_1 varied are shown in Table VII. Clearly, increasing A_1 decreases the deformation energy in spite of the scaling up of the Hamiltonian. Thus, the isoscalar n-p interaction is also responsible for the onset of deformation in the Mo isotopes.

The present results also stress the importance of filling orbitals with good spatial overlap for producing deformation. Table VIII gives the occupation numbers for the $1g_{9/2}$ proton and the $1g_{7/2}$ and $1h_{11/2}$ neutron orbitals for the "realistic" case of $A_0=0.6$, $A_1=0.35$. Both the prolate and

TABLE VI. HFB prolate deformation energies (in MeV) for various values of A_0 ($A_1=0.35$ MeV).

	A_0 (MeV)				
Nucleus	0.0	0.2	0.4	0.6	0.8
^{98}Mo	0	0	0	0	0
^{100}Mo	0	0	0	0.7	2.4
^{102}Mo	0	0	0	1.2	3.4
^{104}Mo	0	0	0.1	1.5	4.2
^{106}Mo	0	0	0.1	1.7	4.8
^{108}Mo	0	0	0.1	1.6	5.1
^{110}Mo	0	0	0.1	1.3	4.8

TABLE VII. HFB prolate deformation energies (in MeV) for various values of A_1 (A_0=0.6 MeV).

	A_1 (MeV)			
Nucleus	0.20	0.35	0.50	0.65
^{98}Mo	0	0	0	0
^{100}Mo	1.3	0.7	0	0
^{102}Mo	1.8	1.2	0.4	0
^{104}Mo	2.5	1.5	0.8	0.1
^{106}Mo	2.6	1.7	0.9	0.4
^{108}Mo	2.3	1.6	0.9	0.4
^{110}Mo	1.9	1.3	0.6	0.3

spherical results are shown. For all of the isotopes considered, the $1g_{9/2}$ proton orbital is more occupied in the prolate solution than in the spherical solution and, moreover, the $1g_{9/2}$ proton occupation numbers follow the deformation energy closely as a function of the neutron number (see Table VI). Through $A=104$, the $1g_{7/2}$ neutron occupation numbers also follow the deformation energy closely. Beyond $A=104$, $1g_{7/2}$ neutrons seem to play a gradually less important role in producing deformation. At this point, however, the $1h_{11/2}$ neutron occupation numbers become large and produce the necessary spatial n-p correlations for deformation to continue. Note that the $1h_{11/2}$ neutron and $1g_{9/2}$ proton orbitals also satisfy the deShalit-Goldhaber criteria for strongly overlapping orbitals.

V. DISCUSSION OF DEFORMATION IN LIGHT AND HEAVY NUCLEI

A. Deformation in the (2s, 1d) shell

In 1962 Talmi and Unna pointed out the important role played by the $1d_{5/2}$ and $1d_{3/2}$ spin-orbit-partner orbitals in building up the spatial correlations necessary for deformation in the $(2s, 1d)$ shell.[4] They showed that, although the $1d_{3/2}$ orbital is unnecessary for a description of the low-lying states of the oxygen isotopes (with only valence neutrons), it admixes very strongly when both valence neutrons and protons are present.

TABLE IX. Effective interaction matrix elements for the $(2s, 1d)$ shell.[a]

j_1	j_2	j_3	j_4	JT	$\langle j_1j_2(JT)\lvert V_{\rm eff}\rvert j_3j_4(JT)\rangle$ (in MeV)
$d_{5/2}$	$d_{5/2}$	$d_{5/2}$	$d_{5/2}$	01	−2.44
$d_{5/2}$	$d_{5/2}$	$d_{5/2}$	$d_{5/2}$	50	−3.66
$d_{5/2}$	$d_{3/2}$	$d_{5/2}$	$d_{3/2}$	10	−5.83
$d_{5/2}$	$d_{5/2}$	$d_{5/2}$	$d_{3/2}$	10	3.17

[a] From Ref. 28.

The crucial role played in this case by the isoscalar n-p interaction between nucleons in the $1d_{5/2}$ and $1d_{3/2}$ partner orbitals can be best appreciated by considering some relevant effective matrix elements. The ones listed in Table IX were obtained by Kuo,[28] but their features are the same for other interactions. Note that the diagonal interaction between $1d_{5/2}$ and $1d_{3/2}$ nucleons in a relative $J=1$, $T=0$ configuration is very strong and, moreover, it is significantly stronger than the attraction between two $1d_{5/2}$ nucleons either in the $J=0$, $T=1$ paired configuration or the $J=5$, $T=0$ stretch configuration. Similarly, the off-diagonal matrix element

$$\langle 1d_{5/2}{}^2(10)\lvert V_{\rm eff}\rvert 1d_{5/2}1d_{3/2}(10)\rangle$$

is very strong, and provides the mechanism for the strong mixing of the $1d_{3/2}$ orbital into the ground states of $(2s, 1d)$-shell nuclei with both valence neutrons and valence protons.

It is important to bear in mind that in the $(2s, 1d)$ shell neutrons and protons can fill the same orbitals, and thus also experience the strong attraction associated with such configurations. For example, from Table IX, we see that the attraction between two $1d_{5/2}$ nucleons in the $J=5$, $T=0$ stretch configuration is also very strong. This situation should be contrasted with the situation in the Zr-Mo region, where neutrons and protons fill different major shells. It is reasonable to expect that deformation should be easier to produce in the $(2s, 1d)$ shell than in the Zr-Mo

TABLE VIII. HFB occupation numbers (SDI parameters: A_0=0.6 MeV, A_1=0.35 MeV).

	$1g_{9/2}$ protons		$1g_{7/2}$ neutrons		$1h_{11/2}$ neutrons	
Nucleus	spherical	prolate	spherical	prolate	spherical	prolate
^{98}Mo	2.63	2.64	0	0	0	0
^{100}Mo	2.63	2.83	0.51	0.70	0.29	0.01
^{102}Mo	2.62	2.95	1.22	1.52	0.69	0.52
^{104}Mo	2.62	3.05	2.02	2.28	1.17	1.22
^{106}Mo	2.62	3.12	2.84	2.89	1.73	2.22
^{108}Mo	2.62	3.15	3.68	3.46	2.39	3.33
^{110}Mo	2.62	3.14	4.47	4.07	3.17	4.33

region, because of the additional possibility of strong correlations between neutrons and protons in the same orbitals. This feature is in fact out both by experimental data and calculations. In the $(2s, 1d)$ shell a well-defined rotational band already occurs in ^{20}Ne, with only two valence neutrons and two valence protons. According to the present calculations, the ^{98}Zr nucleus, which has the same number of valence nucleons as ^{20}Ne, does not exhibit an excited rotational band built on the collective 0.85 MeV 0^+ level.

Finally, it is of interest to see whether the recent observation of a deformed shape for the nucleus ^{32}Mg (Ref. 29) can be included in the picture we have presented. Naive considerations would view ^{32}Mg as having a closed $(N=20)$ neutron shell, which would seem to contradict the present description in which deformation is attributed to the n-p interaction. More careful analysis shows this not to be the case. The lowest neutron orbital above the $(2s, 1d)$ shell is the $1f_{7/2}$. But the deShalit-Goldhaber rule suggests that the orbitals of $1f_{7/2}$ neutrons and $1d_{5/2}$ protons overlap well and therefore interact strongly, effectively lowering the $1f_{7/2}$ neutron orbital. This effect is strongly exhibited by the Nilsson scheme. For $\delta=0.3$ the lowest $K=\frac{1}{2}^-$ orbit from the $(2p, 1f)$ shell crosses with the uppermost orbit from the $(2s, 1d)$ shell.[30] Thus, in ^{32}Mg the appearance of deformation is most probably related to the strong n-p attraction between $1d_{5/2}$ protons and $1f_{7/2}$ neutrons, consistent with the present picture.

B. Deformation in heavy nuclei

The picture that has emerged from studies of both light and medium-weight deformed nuclei is that nuclear shapes are governed by a competition between the isovector pairing interaction which favors sphericity and the isoscalar n-p interaction (isospin pairing) which favors deformation. For a nucleus to deform, the $T=0$ n-p interaction must dominate over the $T=1$ pairing interaction. In light and medium-weight nuclei, where shell effects are important and limit the numbers of valence neutrons and protons, this can occur only when the neutrons and protons fill orbits with very good spatial overlap, so that the n-p matrix elements are strong enough to dominate over the n-n and p-p pairing matrix elements. This effect shows up for instance in the Zr isotopes, where, as seen in Sec. III, deformation would not occur were it not for the simultaneous filling of the $1g_{9/2}$ and $1g_{7/2}$ partner orbitals by protons and neutrons.

In heavier nuclei, the situation is somewhat different. Here there are many close-lying orbitals for both neutrons and protons, and shell effects are less important. Thus, although the interaction between an arbitrary neutron-proton pair may not be as strong as the pairing interaction, the $(n$-$p)$ interaction may still dominate over the pairing interaction if there are a sufficiently large number of valence protons and neutrons. The reason for this is simple. The pairing interaction contributes to the total energy an amount that is roughly proportional to the number of valence protons plus neutrons (N_p+N_n). The n-p interaction can, however, be felt reasonably strongly by any pair of neutrons and protons, so that it contributes to the total energy an amount roughly proportional to $(N_p \times N_n)$. Thus, even though the n-p interaction is not in general as strong as the pairing interaction,[31] it can dominate for sufficiently large N_p and N_n. Moreover, there are strongly overlapping neutron and proton orbitals which are available for valence nucleons in heavy nuclei, most notably the $1h_{11/2}$ proton and $1h_{9/2}$ neutron orbitals in the rare-earth region, and the $1i_{13/2}$ proton and $1i_{11/2}$ neutron orbitals in the transuranic region. Qualitatively these partner orbitals begin to fill very near the observed onsets of deformation in the two heavy regions.[10] Nevertheless, the effect of partner orbitals may be not as crucial for deformation in heavy nuclei as for the lighter $(2s, 1d)$ shell and Zr-Mo deformed regions, because of the above considerations. A better understanding of the relative importance of these partner orbitals and of the general buildup of single-particle orbitals for producing deformation in heavy nuclei requires further quantitative investigation.

In this regard, it is of interest to see whether the view developed in this work can be discussed in relation to the interacting boson approximation (IBA), which has recently been applied successfully to heavy nuclei.[9] In this model, the basic building blocks are pairs of particles in either an $L=0$ (s boson) or an $L=2$ (d boson) state. Separate s and d bosons are assumed for neutrons and protons. These bosons are thought to be the eigenstates of the two-neutron and two-proton Hamiltonians, respectively. In a system with several bosons, the bosons are permitted to interact with one another through an interaction which takes place primarily between neutron and proton bosons and which is usually assumed (for simplicity) to be of a quadrupole-quadrupole form. The IBA has been recently applied to the shape transition exhibited by the Sm isotopes.[32]

Clearly, the simple IBA as described above cannot describe the shape transition in the Zr isotopes. Here, a proper description of the shape transition involves two s bosons for both the protons and the neutrons. One is just the lowest eigenstate of the pairing interaction, whereas the other is a linear combination of the various pairing eigenstates of the diagonalized $J=0^+$ shell-model configurations. This second boson gradually develops correlations as neutrons and protons are added. Apparently, it is the linear combination of pairing eigenstates which best experiences the n-p interaction. In ^{98}Zr, this deformed s boson is quite admixed for the neutrons, involving the $(s_{1/2}{}^2)$, $(g_{7/2}{}^2)$, and $(d_{3/2}{}^2)$ configurations, $(g_{7/2}{}^2)$ being the predominant one. For the protons, because of shell effects, it is mainly of $(g_{9/2}{}^2)$ character, with small admixtures of $(p_{1/2}{}^2)$ and $(d_{5/2}{}^2)$.

In heavy nuclei there are a very large number of close-lying single-particle orbitals, and therefore the eigenvalues of the two-neutron and two-proton systems exhibit large pairing gaps. Thus, in heavy nuclei, the lowest eigenstates of H_{nn} and H_{pp} for the two-particle systems are well separated in energy from the remaining eigenstates and may retain their structure even when many bosons are present.[33]

The above remarks provide some microscopic justification for the IBA in heavy nuclei. However, if the IBA is to develop into a practical approach in light and medium-weight nuclei as well, it seems likely that additional bosons must be included, perhaps additional s and d bosons or a neutron-proton boson.[34]

To conclude, we summarize the main features of the unified description of nuclear deformation presented in this work.

Nuclear deformation is produced by the isoscalar part of the n-p interaction throughout the periodic table. Deformed shapes set in when the pairing interaction (which favors sphericity) is overpowered by the isoscalar interaction between neutrons and protons. When shell effects are important, as in the light $(2s, 1d)$ shell and in the medium-weight Zr-Mo isotopes, the occupation of neutrons and protons of spin-orbit partner orbitals plays a crucial role in determining the onset of deformation. In the heavy rare-earth and transuranic regions, the absence of shell effects makes the role of partner orbitals less crucial.

ACKNOWLEDGMENTS

We would like to thank S. S. M. Wong without whom the shell-model calculations reported in this paper would not have been possible. We also wish to express our appreciation to A. Arima, H. Feshbach, J. Flores, F. Iachello, H. Selic, and K. Sistemich for enlightening comments and discussion, and to I. Talmi for pointing out the Zr-Mo data to us. Finally, one of the authors (P. F.) acknowledges the hospitality of the Bartol Research Foundation and the University of Delaware during several visits, while the other author (S. P.) is grateful for the hospitality provided by IFUNAM. This work was supported in part by CONACYT (PNCB 081) and in part by NSF (INT 77-21522).

[1]E. Cheifetz, R. C. Jared, S. G. Thompson, and J. B. Wilhelmy, Phys. Rev. Lett. 25, 38 (1970).

[2]B. R. Mottelson, in *Proceedings of the International School of Physics "Enrico Fermi" Course XV, Varenna, 1960,* edited by G. Racah (Academic, New York, 1962), p. 44.

[3]A. DeShalit and M. Goldhaber, Phys. Rev. 92, 1211 (1953).

[4]I. Talmi, Rev. Mod. Phys. 34, 704 (1962); I. Unna, Phys. Rev. 132, 2225 (1963).

[5]P. Federman and S. Pittel, Phys. Lett. 77B, 29 (1978).

[6]S. C. K. Nair, A. Ansari, and L. Satpathy, Phys. Lett. 71B, 257 (1977).

[7]F. Ajzenberg-Selove, Nucl. Phys. A190, 1 (1972).

[8]G. E. Brown and A. M. Green, Nucl. Phys. 75, 401 (1966); 85, 87 (1966); P. Federman and I. Talmi, Phys. Lett. 19, 490 (1965); P. Federman, Nucl. Phys. A95, 443 (1967).

[9]A. Arima and F. Iachello, Phys. Rev. Lett. 35, 1069 (1975); Ann. Phys. (N.Y.) 99, 253 (1976); A. Arima, T. Otsuka, F. Iachello, and I. Talmi, Phys. Lett. 66B, 205 (1977); T. Otsuka, A. Arima, F. Iachello, and I. Talmi, *ibid.* 76B, 139 (1978).

[10]P. Federman and S. Pittel, Phys. Lett. 69B, 385 (1977).

[11]P. Federman, S. Pittel, and R. Campos, Phys. Lett. 82B, 9 (1979).

[12]N. Auerbach and I. Talmi, Nucl. Phys. 64, 458 (1965); D. H. Gloeckner, *ibid* A253, 301 (1975).

[13]K. Sistemich, G. Sadler, T. A. Khan, H. Lawin, W. D. Louppe, H. A. Selic, F. Schussler, J. Blachot, E. Monnand, J. P. Becquet, and B. Pfeiffer, Z. Phys. A281, 169 (1977).

[14]T. A. Khan, W. D. Louppe, K. Sistemich, H. Lawin, G. Sadler, and H. A. Selic, Z. Phys. A283, 105 (1977).

[15]B. M. Preedom, E. Newman, and J. C. Hiebert, Phys. Rev. 166, 1156 (1968).

[16]D. C. Slater, E. R. Cosman, and D. J. Pullen, Nucl. Phys. A206, 433 (1973).

[17]C. R. Bingham and M. L. Halbert, Phys. Rev. C 2, 2297 (1970).

[18]J. B. Moorehead and R. A. Moyer, Phys. Rev. 184, 1205 (1969).

[19]N. Auerbach and J. P. Vary, Phys. Rev. C 13, 1709 (1976).

[20] J. Picard and G. Bassani, Nucl. Phys. A131, 636 (1969).

[21] K. Sistemich and H. Selic, private communication.

[22] R. K. Sheline, I. Ragnarsson, and S. G. Nilsson, Phys. Lett. 41B, 115 (1972).

[23] P. Federman, D. H. Feng, S. Pittel, and M. Vallieres, work in progress.

[24] N. Kaffrell, G. Franz, G. Klein, K. Sümmerer, G. Tittle, N. Trautmann, G. Herrmann, and H. Ahrens, in *Proceedings of the 3rd International Conference on Nuclei Far From Stability, Cargèse, 1976,* edited by R. Klapisch (CERN, Geneva, 1976), p. 483.

[25] M. Baranger, in *Cargèse Lectures in Theoretical Physics*, edited by M. Lévy (Benjamin, New York, 1963); A. L. Goodman, *Advances in Nuclear Physics* (Plenum, New York, 1979), Vol. 11, p. 263.

[26] I. M. Green and S. A. Moszkowski, Phys. Rev. 139, B790 (1965).

[27] D. H. Gloeckner and F. J. D. Serduke, Nucl. Phys. A220, 477 (1974).

[28] T. T. S. Kuo, Nucl. Phys. A103, 71 (1967).

[29] R. Klapisch, as referred to by T. E. O. Ericson, in *Proceedings of the International Conference on Nuclear Structure, Tokyo, 1977,* edited by T. Marumori [J. Phys. Soc. Jpn. 44, (1978), Suppl. p. 27].

[30] S. G. Nilsson, Mat. Fys. Medd. Dan. Vid. Selsk. 29, No. 16 (1955).

[31] This remark is true even though Pauli effects in general lead to average interactions stronger for $T=0$ than for $T=1$, as *H.* Feshbach repeatedly pointed out to us during the 1st and 2nd Oaxtepec Symposia on Nuclear Physics.

[32] A. Arima, T. Otsuka, F. Iachello, O. Scholten, and I. Talmi, *Proceedings of the International Conference on Nuclear Structure, Tokyo, 1977,* edited by T. Marumori [J. Phys. Soc. Jpn. 44, (1978), Suppl. p. 509].

[33] F. Iachello, private communication.

[34] The idea of including a neutron-proton boson in the IBA emerged from a discussion with M. Fortes. This possibility is being investigated.